ISSN 1070-3632, Russian Journal of General Chemistry, 2013, Vol. 83, No. 11, pp. 2217–2221. © Pleiades Publishing, Ltd., 2013.
Original Russian Text © A.L. Pirozerskii, E.V. Charnaya, A.I. Nedbai, P.V. Velikorussov, E.V. Shevchenko, M.I. Samoilovich, A.S. Bugaev, 2012, published in Rossiiskii Khimicheskii Zhurnal, 2012, Vol. 56, Nos. 1–2, pp. 96–99.

Influence of the Fractality of Opal Matrices on Melting and Crystallization of Decane in Pores

A. L. Pirozerskii[a], E. V. Charnaya[a], A. I. Nedbai[a], P. V. Velikorussov[a], E. V. Shevchenko[a], M. I. Samoilovich[b], and A. S. Bugaev[c]

[a] *St. Petersburg State University, Universitetskaya nab. 7−9, St. Petersburg, 199034 Russia*
e-mail: charnaya@mail.ru

[b] *Tekhnomash Central Research Institute of Technology, ul. Ivana Franko 4, Moscow, 121108 Russia*
e-mail: samoylovich@technomash.ru

[c] *Moscow Institute of Physics and Technology (State University), Institutskii per. 9, Dolgoprudnyi, Moscow oblast, 141700 Russia*
e-mail: bugaev@cos.ru

Received June 1, 2012

Abstract—In this paper we present the results of studies on melting and crystallization of decane embedded in the pores of opal matrices filled with chemically pure hexadecane. In this studies measured the ultrasonic velocity by the pulse-interference method at frequencies of about 7 MHz in the temperature range 170–290 K.

DOI: 10.1134/S107036321311042X

In the past few years, there has been an outburst of interest in the physical properties on nanocomposites on the basis of mesoporous matrices filled with different substances. Mesoporous matrices used for fabrication of nanocomposites vary in the size, geometry, and connectivity of pore network, degree of pore ordering, and thickness of pore walls. The greatest acceptance has been received by porous silicate glasses, porous alumina, molecular sieves, zeolites, and opal matrices.

Opal matrices have (photonic crystals) attracted particular attention since they possess a system of regularly ordered open pores formed due to dense packing and subsequent sintering of silica spheres about a wavelength of light in diameter. The porosity of unfilled opal matrices is usually close to a porosity corresponding to an ideally dense packing (~26%). However, porosity can be much increased by opening second-order pores between spheres of a smaller diameter which form the basicsilica spheres [1]. As expected, the opening of second-order pores will strongly affect the properties of opal-matrix nanocomposites. In particular, some changes in phase transitions of substances embedded in pores are possible.

There is abundant experimental evidence showing that the melting point of a material embedded in nanometer-sized pores is shifted with respect to that of the bulk materials, and, therewith, the value and sign of this shift depend on the size of the embedded particles and on the ratio of the surface tension coefficients of the liquid and solid phases of the particles and matrix. Furthermore, a considerable broadening of the melting and crystallization ranges together with a wide temperature hysteresis on heating and cooling of nanocomposites were observed. In such a case, the opening of second-order pores in opal matrices should definitely affect both the shifts of melting and crystallization points and the degree of broadening of phase transitions. However, experimental work on such effects has never been done.

In the present publication we report the results of research on the melting–crystallization phase transition of decane embedded in the pores of opal matrices before and after opening of second-order pores. The research was performed by an ultrasonic method which offers substantial advantages over other experimental techniques for studying phase transitions in confined geometry [2]. Previously the melting of decane in confined geometry was studied by differential scanning calorimetry in silica samples with 8.5-nm pores [3], as well as by acoustic methods in porous glass samples [4].

We studied nanocomposites obtained by embedding chemically pure decane in the pores of opal matrices. The starting opal matrix was a cubic close packing of X-ray amorphous silica spheres (diameter ~260 nm) with octahedral and tetrahedral pores between them (first-order pores). In their turn, the SiO_2 spheres consist of smaller diameter spheres (second-order spheres). The porosity of the starting opal matrix was 27%. Treatment with alkali increased porosity to about 44% due to second-order pore opening. Additional smaller diameter pores relate to the fractal structure of opal matrices [1].

The melting point of bulk decane is 245.25 K. Decane completely wets the surface of silicate glass and is scarcely soluble in water.

In our experiments, liquid decane was embedded in porous matrices at room temperature. The samples were parallelepipedal blocks ~0.5 cm^3 in volume.

We measured temperature dependences of the relative changes of ultrasonic velocity $\Delta v/v = [v(T) - v_0]/v_0$ in the heating–cooling cycles in the temperature range 165–295 K. The measurements were performed by the pulse-interference method [5] using longitudinal acoustic waves of about 7 MHz. Signals from two acoustic pulses were compared: one reflected from the front face of a sample and the other passed through the sample one time. At room temperature we measured the absolute velocity of acoustic waves in the samples. The errors in the temperature and temperature gradient in a sample were no larger than 0.2 K and 0.1 K cm^{-1}, respectively. The temperature ramp was no more than 15–20 K h^{-1}, and it decreased to 5 K h^{-1} in and around phase transitions. The acoustic contact of samples with acoustic ducts was provided by means of Apiezon N.

The resulting temperature dependences are presented in Fig. 1. The temperature cycles correspond to cooling of a sample from room temperature (liquid decane) to 165 K (much lower that the temperature of complete crystallization of decane) followed by heating to the initial temperature.

As follows from Fig. 1, the melting and crystallization of decane in pores give rise to strong and nonlinear changes in ultrasonic velocity. Such acoustic anomalies are usually associated with liquid–solid transitions for a substance embedded in mesopores. The temperature dependences of ultrasonic velocity, obtained on sample cooling and heating, are different and are characterized by a hysteresis loop. As seen from Fig. 1a, the steepest rise of ultrasonic velocity during decane crystallization in pores is observed in a narrow temperature range. The average crystallization

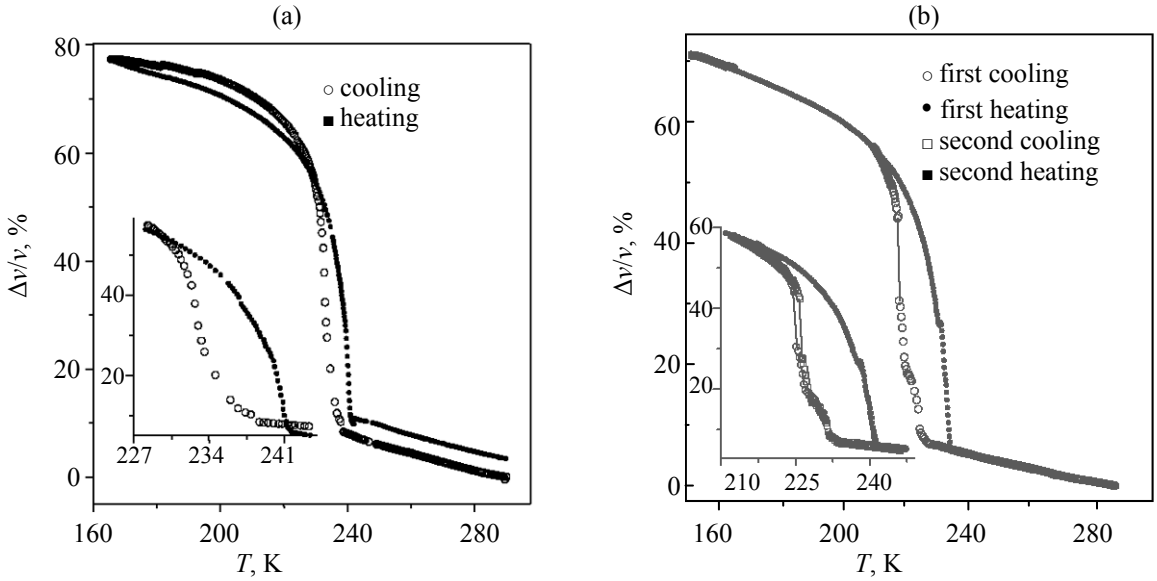

Fig. 1. Temperature dependences of the relative change of longitudinal ultrasonic velocity in the cooling–heating cycle for melting and crystallization of decane in the pores of the (a) starting opal matrix and (b) starting opal matrix treated with alkali. The insert in Fig. 1a shows the hysteresis curve corresponding to crystallization and melting of decane in pores. The insert in Fig. 1b shows the changes in the ultrasonic velocity in the narrow temperature range corresponding to the crystallization–melting phase transition of decane in pores, for two successive temperature cycles. The straight lines relate to a fast change of ultrasonic velocity on decane crystallization.

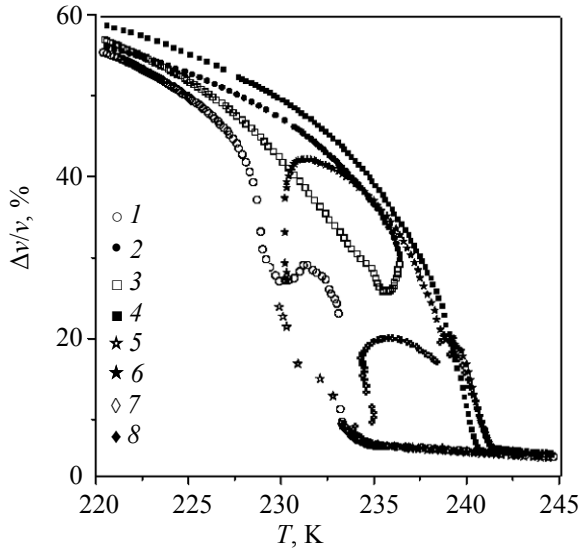

Fig. 2. Temperature dependences of the relative change of longitudinal ultrasonic velocity in partial cooling–heating cycles for the opal matrix with open second-order pores filled with decane: (*1*) first cooling; (*2*) first heating; (*3*) second cooling; (*4*) second heating; (*5*) third cooling; (*6*) third heating; (*7*) fourth cooling; and (*8*) fourth heating.

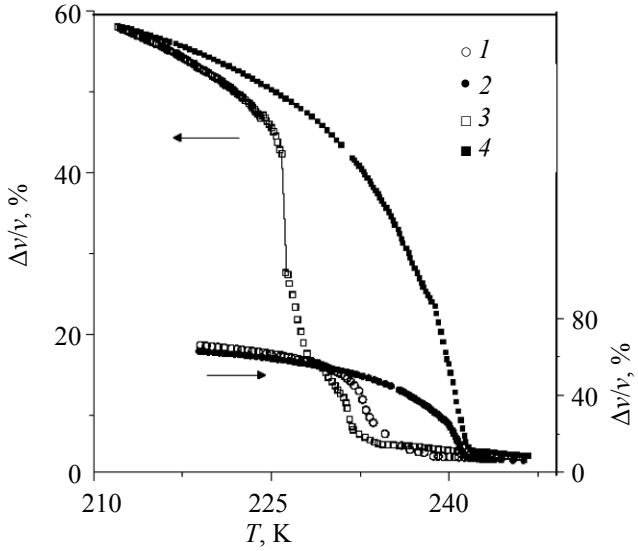

Fig. 3. Comparison of the temperature dependences of the relative change of ultrasonic velocity in the decane-filled (circles) starting opal matrix and (squares) matrix with open second-order pores: (*1*) cooling; (*2*) heating; (*3*) starting sample, cooling; and (*4*) starting sample, heating. The straight line relates to a fast change of ultrasonic velocity on decane crystallization.

point of decane in pores was estimated at 233 K. The curves of the relative changes of ultrasonic velocity merge at about 230 K, which corresponds to complete crystalization in the most volume of pores filled with decan.

The opposite process, viz. a decrease of ultrasonic velocity on sample heating, takes place in a slightly broader temperature range. The closing of the hysteresis loops of the ultrasonic velocity and flattening of its temperature dependence upon of heating correspond to complete melting of decane in pores. The average melting point of decane in pores was estimated at 240 K. Note that the divergence of the velocity curves at heating and cooling, observed below 230 K, seems to be associated with residual mechanical stresses arising in the sample on thermal cycling.

Figure 1b shows the temperature dependences of the relative change of longitudinal ultrasonic velocity in a decane-filled opal matrix subjected to additional treatment in an alkali solution. The hysteresis loop between the velocity curves corresponding to decane melting and crystallization in this sample has become much larger. Moreover, the temperature ranges of decane melting and crystallization, too, have extended, and the temperature dependences of the velocity have acquired two well-defined steps which are especially pronounced for crystallization. Noteworthy is an almost full reproducibility of experimental data in the first and second measurement cycles.

Figure 2 shows the temperature dependences of the relative change of ultrasonic velocity for a decane-filled opal matrix treated with alkali, for partial cooling–heating cycles, when heating (cooling) started before completion of the crystallization (melting) process. The measurements were performed in the range from room temperature to 190 K (for clarity, in Fig. 2 we only show the results obtained at 220–245 K).

The experiments with partial temperature cycles evidenced that the crystallization process is completely irreversible and the melting process is partially reversible (cycles 2–4). Moreover, these experiments revealed two independent crystallization processes which correspond to two steps in the temperature dependence of ultrasonic velocity. Actually, in the third cycle heating is initiated below the temperature range of the first step in the velocity curve at crystallization. Crystallization of decane still continues when the sample is heated, and the velocity curve gets closer to the curve obtained for the cooling–heating cycle in the vicinity of the second (low-temperature) step

corresponding to decane melting. In the fourth cycle, heating is initiated at the very beginning of crystallization. Therewith, crystallization only spans the range, where the first (high-tem-perature) step for melting is observed.

The data obtained show that the temperature range corresponding to melting of decane in nanopores is lower compared to the melting point of bulk decane, and this relates both to the starting opal matrix and to that with open second-order pores. The fact that the melting point of decane confined to the pores of the alkali-treated matrix is even more decreased than in the case of the starting opal matrix can be explained in terms of the opening of second-order pores due to alkali treatment. Comparison of the data presented in Fig. 1 shows that the first (high-temperature) step in the velocity curve for cooling corresponds to the crystallization range for the starting sample. For clarity, the velocity data for the starting and treated samples in Fig. 3 are presented on different scales.

Thus, we can suggest that the two steps in the temperature dependence of ultrasonic velocity for the sample with open second-order pores are associated with crystallization and melting of decane in the pores between first- and second-order silica spheres. According to Fig. 2, the crystallization and melting processes in the first- and second-order pores occur fairly independently of one another.

The virtually complete reproducibility of the experimental results for different crystallization–melting cycles of decane in pores shows that both the melting and crystallization points are controlled by the geometry and structure of the pores. The reproducibility of the crystallization process is probably explained by the fact that crystallization is induced by heterogeneous nucleation. In terms of this suggestion, the presence of hysteresis between the melting and crystallization curves implies that heterogeneous crystallization in a supercooled liquid intensifies only below some specific temperature point, when, for instance, the critical radius of a nucleus gets smaller than the pore size.

The average melting point of decane in the pores of the starting opal matrix is close to 240 K. The same temperature corresponds to the higher temperature part of the melting curve for the sample with open second-order pores (Fig. 2). This temperature is assignable to melting of decane in the pores between first-order silica spheres. The lower temperature step on the melting curve is near 232 K. This step is assignable to melting of decane in the pores between second-order spheres.

The fact that decane embedded in the pores of opal matrices has a decreased melting point is consistent with the previous observations on the behavior of other organic liquid, as well as metals embedded in nanoporous matrices. The shifts of the melting points of nanoparticles under confined geometry are usually interpreted in terms of thermodynamic models for isolated spherical particles (see, for example, [6] and references therein), including that based on the Gibbs–Thomson equation. This theory gives the following equation for shift of the melting point of a small particle $\Delta T = T_m - T_b$:

$$\frac{\Delta T}{T_b} = -\frac{2\gamma_{sl}}{L\rho R},$$

where T_b and T_m are the melting points of the bulk material and the particle, respectively; γ_{sl}, surface tension at the solid–liquid interface; L, latent heat of melting; ρ, particle density; and R, particle radius.

This equation predicts a linear dependence of the shift of the melting point of a small particle on the reciprocal radius, which agrees with a lower melting point of decane confined to the pores between second-order silica spheres.

Assuming that the shift of the melting point of decane is linearly related to pore size, as well as that the size of pores between first- and second-order pores is proportional to the size D of basic silica spheres, we can estimate the size of second-order pores. Actually, for the pores between first-order spheres we can write down the following equation which follows from Eq. (1): $\Delta T = k/D$, where k is the proportionality factor between the melting point shift and the reciprocal size of silica spheres. Using the data obtained, k was estimated at 1350 K nm. With this k value, the size of second-order spheres could be estimated at 100 nm. However, this value seems to be overestimated [1]. A possible reason is the size of the second-order pores formed due to alkaline treatment is not proportional to the size of second-order silica spheres in the starting opal matrix.

Thus, the experimental studies on melting and crystallization of decane embedded in the pores of opal matrices revealed an effect of opening of second-order

pores on the shift of its melting point with respect to the melting point of bulk decane and on the temperature hysteresis on melting and crystallization of decane in pores.

REFERENCES

1. Masalov, V.M., Sukhinina, N.S., Kudrenko, E.A., and Emelchenko, G.A., *Nanotechnology*, 2011, vol. 22, p. 275718.
2. Charnaya, E.V., *Acoust. Phys*., 2008, vol. 54, no. 6, p. 802.
3. Jackson, C.L. and McKenna, G.B., *J. Chem. Phys*., 1990, vol. 93, p. 9002.
4. Borisov, B.F., Gartvik, A.V., Gorchakov, A.G., and Charnaya, E.V., *Phys. Solid State*, 2009, vol. 51, p. 823.
5. Gitis, M.B., Mikhailov, I.G., and Shutilov, V.A., *Akust. Zh*., 1969, vol. 15, p. 28.